Phys. Med. Biol. **44** (1999) R1–R22. Printed in the UK PII: S0031-9155(99)74209-0

TOPICAL REVIEW

Review of photon interaction cross section data in the medical and biological context*

J H Hubbell†
11830 Rocking Horse Road, Rockville, MD 20852, USA

Received 13 August 1998

Abstract. The probability of a photon (x-ray, gamma-ray, bremsstrahlung, etc) of a given energy E undergoing absorption or scattering when traversing a layer of material Z can be expressed quantitatively in terms of a linear attenuation coefficient μ (cm^{-1}). Since μ is dependent on the material's density, ρ (g cm^{-3}), which can be variable, the quantity usually tabulated is the mass attenuation coefficient μ/ρ (cm^2 g^{-1}) in which the dependence on the density has been removed. μ/ρ, in turn, can be obtained as the sum of the different types of possible interactions of photons with atoms of the material. For photon energies below 1 MeV the major interaction processes to be considered are incoherent (Compton) scattering, coherent (Rayleigh) scattering and atomic photoeffect absorption. Above 1 MeV one must also include nuclear-field pair production and atomic-field (triplet) production, and above 5 MeV one in principle should include photonuclear absorption, although the latter is neglected in data tabulations up to the present time. This review includes a selective history of measurements and theory relating to μ/ρ from the turn of the century up to the present time, and is intended to provide a basis for further calculations and critical tabulations of photon cross section data, particularly as required by users in radiation medicine and biology. The mass energy-absorption coefficient μ_{en}/ρ is also briefly discussed.

1. Introduction

In medical physics and in radiation biology, as well as in many other areas of human enterprise, few sets of physical data are as ubiquitous and widely needed and used as data on the transmission and absorption of x-rays in biological, shielding and dosimetric materials.

Within a very few years after the discovery of x-rays by Röntgen (1895), the transmission of a narrow (parallel) beam of x-rays through layers of different materials was measured and quantified with respect to photon‡ incident energy and atomic number of the material by Barkla and Sadler (1907, 1909). This quantification is in terms of the mass attenuation coefficient§

* Work supported by the National Institute of Standards and Technology Office of Standard Reference Data.
† Address for correspondence: National Institute of Standards and Technology, Ionizing Radiation Division, Gaithersburg, MD 20899-8463, USA
‡ In this work the generic term 'photon' will be frequently used, which includes gamma rays, bremsstrahlung and other electromagnetic radiation as well as x-rays.
§ The quantity μ/ρ has often been referred to in the literature (e.g., Allen 1935, 1971/1972, Leroux 1960, Victoreen 1943, 1948, 1949, Liebhafski *et al* 1960, Heinrich 1966, 1986) as the 'mass absorption coefficient'. However, the term 'mass absorption coefficient' has also been used to refer to the mass energy-transfer coefficient (e.g., Evans 1955, 1968) and mass energy-absorption coefficient (e.g., Allison 1961), both having to do with photon energy deposition in the target material. Hence, to avoid confusion, this paper continues to follow the International Commission on Radiation Units and Measurements (ICRU 1980) nomenclature 'mass attenuation coefficient' as used at NBS/NIST by White (1952), White Grodstein (1957) and in subsequent NBS/NIST publications as well as by Leroux and Thinh (1977) to refer to the total probability of the photon interaction processes.

0031-9155/99/010001+22$19.50

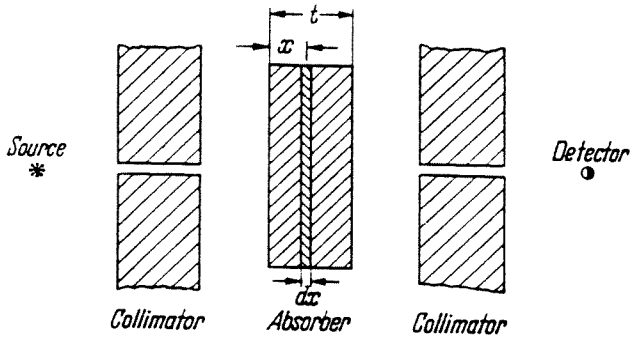

Figure 1. Arrangement for experimental determination of narrow-beam attenuation coefficients. The absorber is a slab of thickness t with plane parallel faces normal to the beam defined by the source, collimators and detector, and dx is a differential layer at distance x into the absorber.

μ/ρ (cm^2 g^{-1}) which can be defined as

$$\mu/\rho = t^{-1} \ln(I_0/I(t)) \tag{1}$$

in which t is the mass thickness of the absorber layer in units of g cm^{-2}. I_0 is the intensity of the incident beam of photons measured with the absorber layer removed from the beam, and $I(t)$ is the intensity of the transmitted beam measured with the absorber interposed as shown schematically in figure 1, in which dx is the thickness of a differential layer at distance x into the absorber. ρ is the density of the absorber layer in g cm^{-3} and μ is the linear attenuation coefficient in cm^{-1}. Since μ is dependent on the sample density ρ which can vary considerably for a given element or compound, for compilation purposes this dependency is removed by tabulating the mass attenuation coefficient μ/ρ.

As described in more detail in Hubbell (1969), the fractional reduction of the beam intensity, $-\mathrm{d}I/I$, is proportional to the above mass attenuation coefficient μ/ρ, and to the layer thickness, dx, i.e.

$$-\mathrm{d}I/I = (\mu/\rho)\,\mathrm{d}x. \tag{2}$$

Integrating this equation, one obtains the intensity $I(t)$ transmitted through the slab

$$I(t) = I_0 \exp\left(-\int_0^t (\mu/\rho)(x)\,\mathrm{d}x \right). \tag{3}$$

For a homogeneous medium, equation (3) reduces to the well-established Bouguer (1729)–Lambert (1760)–Beer (1852) exponential attenuation law

$$I(t) = I_0 \exp[-(\mu/\rho)t] \tag{4}$$

from which equation (1) follows.

Calculations of photon interaction data are generally in terms of atomic cross sections, in units of cm^2/atom, customarily in units of barns/atom (or b/atom) where 1 barn $= 10^{-24}$ cm^2. The total atomic cross section σ_{tot} is thus related to the total mass attenuation coefficient according to

$$\mu/\rho(\mathrm{cm}^2\ \mathrm{g}^{-1}) = \sigma_{\mathrm{tot}}(\mathrm{cm}^2/\mathrm{atom})/(u\ (\mathrm{g})A) = \sigma_{\mathrm{tot}}(\mathrm{b/atom}) \times 10^{-24}/(u\ (\mathrm{g})A) \tag{5}$$

where u(g)(= 1.660 5402 $\times 10^{-24}$ g) (Cohen and Taylor 1986, 1997) is the atomic mass unit, which is defined as 1/12 of the mass of an atom of the nuclide ^{12}C, and A is the relative atomic mass of the target element (Martin 1988). It can be noted that u (g) $= 1/N_A$, where N_A is Avogadro's number (= 6.022 1367 $\times 10^{23}$ atoms/mol).

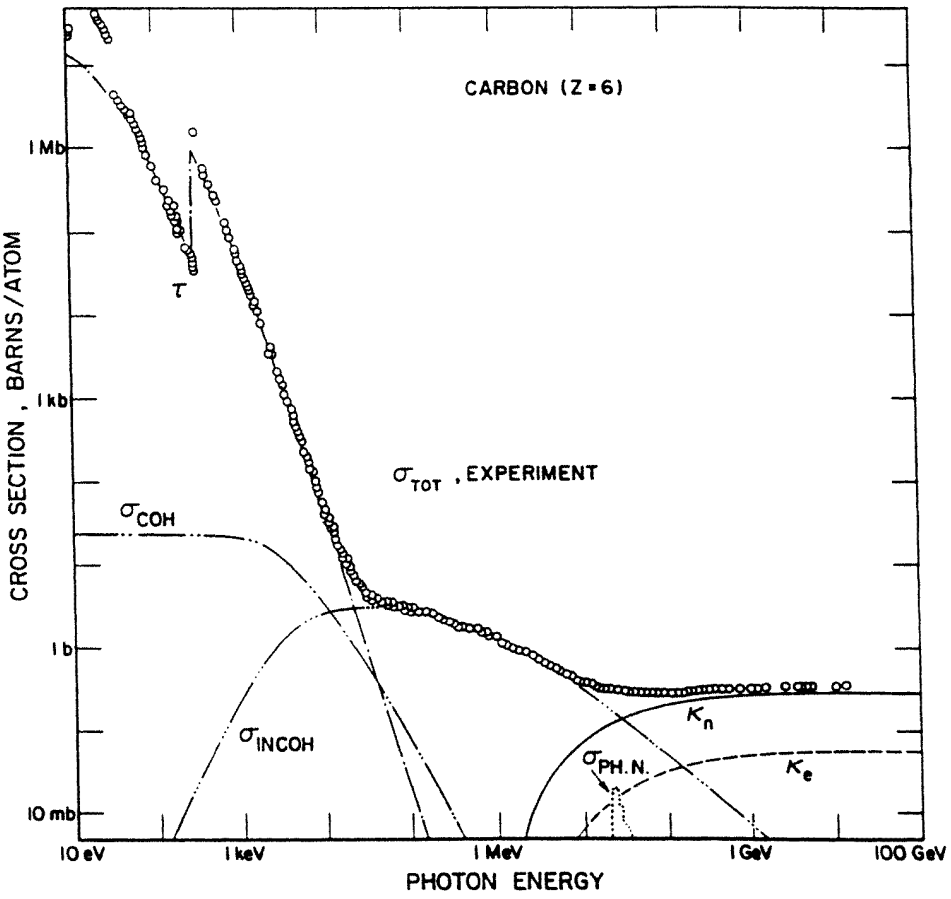

Figure 2. Contributions of atomic photoeffect, τ, coherent scattering, σ_{COH}, incoherent (Compton) scattering, σ_{INCOH}, nuclear-field pair production, κ_n, electron-field pair production (triplet), κ_e, and nuclear photoabsorption, $\sigma_{\mathrm{PH.N.}}$, to the total measured cross section, σ_{TOT} (circles) in carbon over the photon energy range 10 eV to 100 GeV. The measured σ_{TOT} points, taken from 90 independent literature references, are not all shown in regions of high measurement density.

The total atomic cross section σ_{tot} can be written as the sum over the cross sections for the most probable individual processes by which photons interact with atoms

$$\sigma_{\mathrm{tot}} = \sigma_{\mathrm{pe}} + \sigma_{\mathrm{incoh}} + \sigma_{\mathrm{coh}} + \sigma_{\mathrm{pair}} + \sigma_{\mathrm{trip}} + \sigma_{\mathrm{ph.n.}} \tag{6}$$

in which σ_{pe} (or τ) is the atomic photoeffect cross section, σ_{incoh} and σ_{coh} are the incoherent (Compton) and coherent (Rayleigh) cross sections respectively. σ_{pair} (or κ_n) and σ_{trip} (or κ_e) are the cross sections for electron–positron pair production (creation) in the field of the nucleus and in the field of the atomic electrons ('triplet' production) respectively. Finally, $\sigma_{\mathrm{ph.n.}}$ is the nuclear photoeffect cross section discussed in the following paragraphs. All of these individual processes are shown in figures 2 and 3 for C ($Z = 6$) and Pb ($Z = 82$) respectively, from Hubbell *et al* (1980).

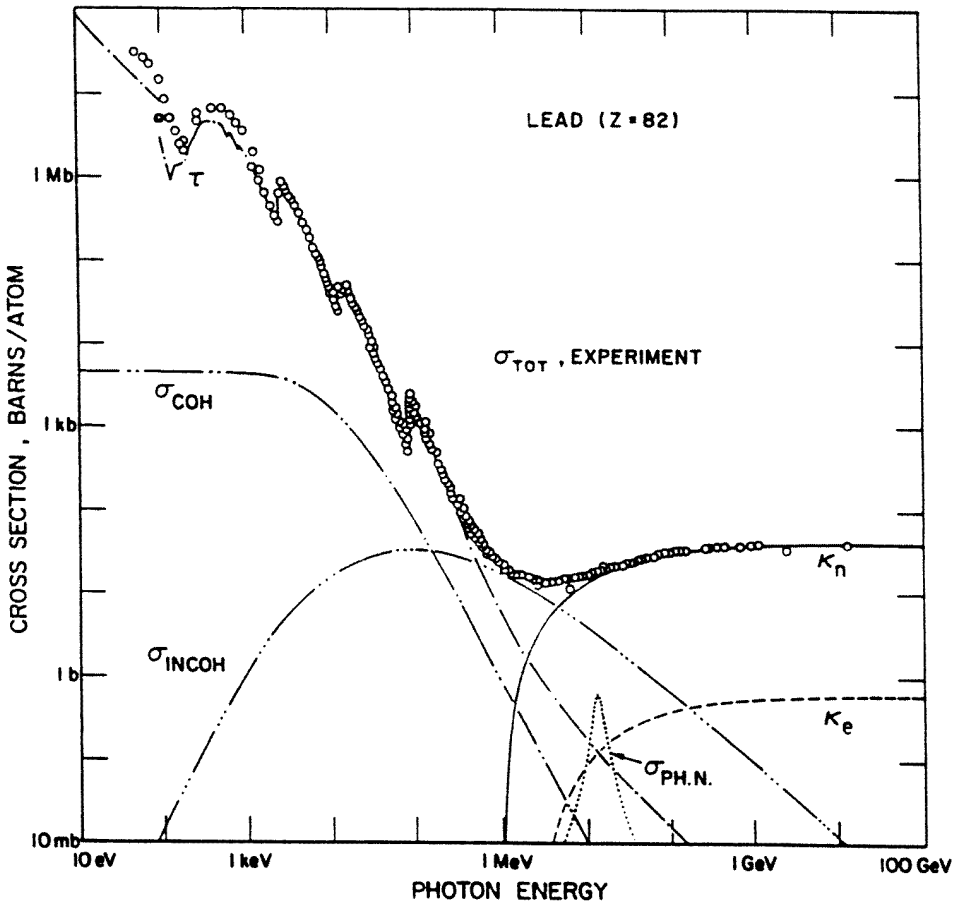

Figure 3. Contributions of atomic photoeffect, τ, coherent scattering, σ_{COH}, incoherent (Compton) scattering, σ_{INCOH}, nuclear-field pair production, κ_n, electron-field pair production (triplet), κ_e, and nuclear photoabsorption, $\sigma_{\mathrm{PH.N.}}$, to the total measured cross section, σ_{TOT} (circles), in lead over the photon energy range 10 eV to 100 GeV. The measured σ_{TOT} points, taken from 121 independent literature references, are not all shown in regions of high measurement density.

1.1. Nuclear photoeffect, $\sigma_{ph.n.}$

In equation (6), the photonuclear cross section $\sigma_{\mathrm{ph.n.}}$ is a measurable effect (see, for example, Gimm and Hubbell 1978). However, this process in which the photon is absorbed by the atomic nucleus and one or more nucleons (neutrons and/or protons) are ejected, is not readily amenable to systematic calculation and tabulation. This is due to a number of factors including its irregular dependence, both shape and magnitude, on both A and Z, and its sensitivity to isotopic abundances in a given sample of an element (see, for example, Hayward 1970, Fuller and Hayward 1976, Dietrich and Berman 1988). Hence, $\sigma_{\mathrm{ph.n.}}$ has been omitted from μ/ρ compilations up to the present, even though at its giant resonance peak between 5 and 40 MeV it can contribute between 2% (high-Z elements) and 6% (low-Z elements) to the total cross section σ_{tot} (see the illustrative tables in Hubbell 1969, 1982).

Hence, current compilations of the mass attenuation coefficient μ/ρ are derived from theoretical or semiempirical values of the cross sections for the individual processes according

to

$$\mu/\rho = (\sigma_{\rm pe} + \sigma_{\rm incoh} + \sigma_{\rm coh} + \sigma_{\rm pair} + \sigma_{\rm trip})/uA \tag{7}$$

referring back to equation (5) for the meaning and units of the conversion factor $1/uA$. The cross sections for the individual processes are discussed in section 3, particularly the cross sections obtained or derived, and used, in the recent compilations by Berger and Hubbell (1987), Creagh and Hubbell (1992), Seltzer (1993), Seltzer and Hubbell (1995), Hubbell and Seltzer (1995), Berger and Hubbell (1998/1999) and by Cullen *et al* (1997).

2. History

For a listing of the available measurements of μ/ρ beginning with the above work of Barkla and Sadler (1907, 1909) up to 1995, for photon energies from 10 eV up to 13.5 GeV in elements $Z = 1$ to 94, one can consult the annotated bibliographies of Hubbell (1994, 1996). From time to time these measurements have been graphically compared with available theory, in order to evaluate the theory for purposes of systematic compilations aimed at medical, biological and other practical applications. Among these evaluations are the graphical comparisons by Hubbell (1971) (10 eV to 100 GeV) and by Saloman *et al* (1988).

The first major compilation of μ/ρ data appears to be that by Allen (1935), covering the photon energy range 30 eV to 2.5 MeV, 32 elements $Z = 1$ to 92 based on his own measurements (for example Allen 1924, 1926), combined with others he found in the literature. First published in the Compton and Allison book (Allen 1935), these tables were soon published thereafter in the Chemical Rubber Handbook, appearing virtually unchanged in all editions up to 1971/1972 (Allen 1971/1972). Since no theory was used in constructing the Allen (1935, 1971/1972) compilation, but only the widely scattered measurements found in the literature, there were wide gaps, requiring extensive interpolation and extrapolation across Z and photon energy in order to use this data base in many practical applications.

In graphing the Allen (1935) μ/ρ data versus Z at constant photon energy to compare with some new measurements (Hubbell 1953), significant departures from Z-smoothness were noted, particularly in the vicinity of Ni ($Z = 28$), in agreement with the very early observation of this anomaly by Barkla and Sadler (1907). These departures from Z-smoothness are attributable to the fact that the relative atomic mass A is not a smooth monotonically increasing function of Z, but depends on the isotopic mix for each element. These mixes, of cosmogenic origin (or since the atomic age altered by isotopic separation, such as for Li), are irregular. The function A versus Z even reverses for the Co(27)–Ni(28)–Cu(29) sequence, as well as for the Ar(18)–K(19)–Ca(20) sequence.

These departures from Z-smoothness (even where atomic photoeffect absorption edge discontinuities (section 3.1) are not involved) have been a limitation on the accuracy of some μ/ρ fitted compilations where Z-smoothness was assumed for interpolation purposes. Such compilations include, for example, those of Leroux (1960), Leroux and Thinh (1977) and Heinrich (1966, 1986). In his later compilation Heinrich (1986) acknowledged this problem, but considered the A-irregularity (versus Z) to be within the spread of the uncertainties of the available measured data to which the compilation was fitted.

Following the work of Allen (1935), the next major μ/ρ compilation was the semiempirical set by Victoreen (1949), based on his evaluations in Victoreen (1943, 1948) making use of the Klein–Nishina formula for total Compton scattering and some interpretation of the atomic photoeffect and its absorption edges using Sommerfeld (1934) theory, as well as available μ/ρ

measured data. Davisson and Evans (1952) published tables for 24 elements $Z = 1$ to 83 and photon energies 102.2 keV to 6.13 MeV (up to 25.54 MeV for $Z = 13$ and 82), obtaining pair production cross sections by graphical integration over the Bethe–Heitler (1934) Born approximation expression.

The National Bureau of Standards (now the National Institute of Standards and Technology) entered this area of collection, evaluation, analysis and compilation of μ/ρ data with the work of Fano (1953), White (1952), White-Grodstein (1957) and McGinnies (now R T Berger) (1959). The White (1952) and White-Grodstein (1957) μ/ρ tables were incorporated into Davisson's (1955, 1965) Chapter II appendix in two editions of the Siegbahn book.

Building on this, White (1952), White-Grodstein (1957) and McGinnies (Berger) (1959) foundation work, new theory and measurements were incorporated by Hubbell and Berger (1968) for tables of μ/ρ and μ_{en}/ρ (μ_{en}/ρ is the mass energy-absorption coefficient, briefly described in section 4) and accompanying text for an invited contribution to the IAEA *Engineering Compendium on Radiation Shielding*. With some additional new material, these tables were published by Hubbell (1969) in the NSRDS-NBS 29 report following their appearance also in the chapter by Evans (1968) in the Attix–Roesch book *Radiation Dosimetry* (2nd edition, vol 1).

At the same time, a collaboration of NBS with the Lawrence Livermore National Laboratory (LLNL) produced extensive tables (McMaster *et al* 1969, 1970, Hubbell *et al* 1974) based on a combination of theoretical and measured data, weighted together, and which provided log–log cubic fitting parameters for the individual component cross sections. This effort was in conjunction and collaboration with the LLNL series of μ/ρ and related tables beginning with Plechaty and Terrall (1966) and extending up through the recent tables by Cullen *et al* (1989, 1997). A somewhat independent tabulation by Storm and Israel (1970), using pair production and some of the scattering data interpolated from NBS, covered all Zs from 1 to 100. Other notable μ/ρ compilations of this period include, for example, the Boeing compilation by Brown (1966) 1 keV to 10 MeV, $Z = 1$ to 100, the extensive parametric fits by Biggs and Lighthill (1971), the 100 eV to 1 MeV, $Z = 1$ to 94 compilation by Veigele (1973) and the radiology-oriented compilation by Johns and Cunningham (1969, 1983).

The discrepancies and envelope of uncertainty of available μ/ρ data have been examined from time to time, including the effects of molecular and ionic chemical binding, particularly in the vicinity of absorption edges (for example Deslattes 1969). More recent efforts at such assessments include the International Union for Crystallography (IUCr) project by Creagh and Hubbell (1987, 1990, 1992) and as reviewed by Gerward (1993).

Interest in low-energy photon attenuation led to tables by Henke *et al* (1967, 1982) for energies 30 eV to 6 and 10 keV, and more recently the tables by Henke *et al* (1993) for photon energies 50 eV to 30 keV, $Z = 1$–92. Responding to low-energy dosimetry standards requirements, Hubbell (1977) developed μ/ρ and μ_{en}/ρ data for a few elements and mixtures of particular dosimetric interest, for the range 100 eV to 20 MeV, and later Hubbell (1982) published tables of μ/ρ and μ_{en}/ρ for 40 elements and 45 mixtures and compounds over the energy range 1 keV to 20 MeV. The latter tables are still widely used as reference values, but should now be replaced by the Berger–Hubbell (1987 (and updates)) XCOM μ/ρ values and the μ_{en}/ρ values of Seltzer (1993) and Hubbell and Seltzer (1995). Extensive new calculations and theoretical tabulations by Chantler (1995) of scattering cross sections and quantities related to μ/ρ have recently become available for photon energies from a few eV up to 1 MeV or less, for $Z = 1$–92. However, it is not yet clear how to incorporate this new source of data into μ/ρ tables for medical, biological and other practical applications.

3. The individual photon interaction processes

3.1. The atomic photoeffect cross section σ_{pe} (or τ)

As discussed and historically reviewed in some detail in Hubbell (1969), in the atomic photoeffect, a photon disappears and an electron is ejected from an atom. The electron carries away all the energy of the absorbed photon, minus the energy binding the electron to the atom. The K-shell electrons, which are the most tightly bound, are the most important in the energy range of medical and biological interest. However, if the photon energy drops below the binding energy of a given shell, an electron from that shell cannot be ejected. Hence, particularly for medium- and high-Z elements, a plot of $\sigma_{\rm pe}$ versus photon energy exhibits the characteristic absorption edges as the binding energy of each electron subshell is attained and a new channel for photoexcitation becomes energetically allowed. Although these absorption edges have superimposed on them some degree of fine structure, discussed in the last paragraph in this section, in medical and other general-purpose attenuation coefficient compilations, these edges are idealized as simple sawtooth shapes.

In the early semitheoretical compilations of μ/ρ, the scattering cross sections were available theoretically to a reasonable approximation from the Klein–Nishina (1929) formula. Thus the photoeffect cross section was obtained by subtracting the theoretical scattering cross sections from measured values of μ/ρ and interpolating across Z and photon energy, taking care to account for the photoeffect absorption edges shifting in energy with Z.

For a more extensive listing of the early calculations of the atomic photoeffect, the reader is referred to Hubbell (1969). Most of these calculations were for the K-shell only, typified by the high-energy work of Pratt (1960) providing the asymptotic behaviour going to arbitrarily high energies and by Pratt *et al* (1964) in the range 200 keV to 2 MeV. Hultberg *et al* (1961, 1968) used the Swedish BESK computer to compute K-shell cross sections, including photoelectron angular distributions, for 21 elements $Z = 1$ to 100 for photon energies extending as low as 1 keV ($Z = 1$) to as high as 10 MeV ($Z = 92$).

A significant breakthrough came with the atomic photoeffect cross section calculations by Rakavy and Ron (1965, 1967) for not only the K shell, but also for all the significantly contributing higher subshells (L_{I-III}, M_{I-V}, N_{I-VII} and O_{I-III}) over the energy range 1 keV to 2 MeV for $Z = 13$, 26, 50, 74 and 92. Other important multishell photoeffect calculations in this time period, which also provide historical reviews of earlier work, are those by Alling and Johnson (1965), Matese and Johnson (1965) and by Schmickley and Pratt (1967). Interpolations from these works, along with the K-shell high-energy asymptotic behaviour provided by Pratt (1960), were helpful in constructing the tables of Hubbell (1969), along with a large body of experimentally determined total photoeffect cross section data obtained by subtracting 'known' theoretical scattering cross sections from measured total cross sections (attenuation coefficients).

A greater breakthrough came with the systematic calculations by Scofield (1973) of the atomic photoeffect cross sections for all subshells, for all elements $Z = 1$ to 101, over the photon energy range 1 keV to 1.5 MeV. These non-relativistic calculations were based on his solution of the Dirac equation for the orbital electrons moving in a static Hartree–Slater central potential. For $Z = 2$ to 54, Scofield (1973) provided renormalization factors to convert to values expected from a relativistic Hartree–Fock model.

This renormalization was performed for two subsequent compilations of μ/ρ and $\mu_{\rm en}/\rho$ by Hubbell (1977, 1982) and by Hubbell *et al* (1980). However, detailed comparisons (Saloman and Hubbell 1986, Saloman *et al* 1988) with the extensive NBS/NIST μ/ρ measurement data base (Hubbell 1971, 1994, 1996, Hubbell *et al* 1986) tend to favour the unrenormalized Scofield

(1973) $\sigma_{\rm pe}$ over the renormalized values. Hence, in subsequent compilations by Berger and Hubbell (1987) and Hubbell and Seltzer (1995), the unrenormalized Scofield (1973) $\sigma_{\rm pe}$ values have been used.

In a private communication to Saloman and Hubbell, Scofield (1985) extended these calculations down to 0.1 keV, and these (unrenormalized values) are also included in the comparison by Saloman and Hubbell (1986) and Saloman *et al* (1988), both numerically and graphically, with the NBS/NIST μ/ρ measurement data base as well as with an experimentally based compilation by Henke *et al* (1982). Values of $\sigma_{\rm pe}$ are also given in the extensive theoretical results of Chantler (1995) computed within a self-consistent Dirac–Hartree–Fock framework, mentioned earlier. For the elements $Z = 1$ to 92, the lower-bound energy varies between 1 and 10 eV, and the upper-bound energy varies between 0.4 and 1.0 MeV. Further detailed comparisons with the NBS/NIST measurement data base are under way to consider whether these values could or should supplant the Scofield (1973, 1985) $\sigma_{\rm pe}$ values in the NIST (for example Hubbell and Seltzer 1995) and LLNL (for example Cullen *et al* 1997) currently disseminated μ/ρ compilations for medical and biological applications.

3.1.1. Absorption-edge fine structure. Oscillatory structures just above absorption edges are well known (for example Sommerfeld 1920, Azároff 1963, Stern 1974) and can be easily observed with high-resolution spectrometers (for example Faessler 1955, Lytle *et al* 1975, Del Grande 1986, 1990). Above some thresholds rather dramatic peaks can occur, due to atomic photoionization resonances. For example, in her μ/ρ measurements just above the K edge for the series of metals Ti ($Z = 22$, $E_{\rm K\text{-}edge} = 4.97$ keV) to Zn ($Z = 30$, $E_{\rm K\text{-}edge} = 9.66$ keV), Del Grande (1986) observed oscillations, confined to within $\sim$0.5 keV above the edge, of the order of $\sim$0.05 keV width with peaks extending $\sim$5% to $\sim$10% above the smoothed theoretical values. Fe ($Z = 26$) and Cu ($Z = 29$) each showed one of the series of narrow peaks to be extending $\sim$20% above the smoothed values.

Superimposed on these can be smaller modulations, of the order of $\sim$2% or less, of extended x-ray absorption fine structure (EXAFS) associated with chemical binding effects. However, due to their dependence on temperature and other variable atomic environments, these and the above oscillatory structures are currently ignored in μ/ρ tabulations for medical and biological applications.

3.2. Incoherent (Compton) and coherent (Rayleigh) scattering, σ_{incoh} and σ_{coh}

3.2.1. Incoherent/Compton/inelastic scattering σ_{incoh}. For up-to-date information on the incoherent (Compton) scattering cross section $\sigma_{\rm incoh}$, attention is here called to a special issue of *Radiation Physics and Chemistry* edited by Bradley (1997) giving collectively a rather comprehensive survey of this topic. The all-invited papers in this issue include an overview of theory by Bergstrom and Pratt (1997), a summary of experiments by Kane (1997), a study of momentum distributions by Cooper (1997), resonant Raman scattering by Manninen (1997), applications in biomedical science and industry by Harding (1997) and an historical and status review by Hubbell (1997).

As mentioned by Bergstrom and Pratt (1997) and earlier in the extensive review by Kane (1992) and in treatments by Bergstrom *et al* (1992, 1993) and Pratt *et al* (1994), relativistic S-matrix calculations are becoming available and will probably supplant the currently used incoherent scattering function $S(x, Z)$ approach, in which x is a momentum transfer variable related to the incident photon energy and the deflection angle of the scattered photon. However, the S-matrix results are not yet particularly 'user-friendly' for medical–biological applications.

Current μ/ρ compilations such as the Berger–Hubbell (1987) XCOM PC program, the Hubbell–Seltzer (1995) tabulation, and the Cullen *et al* (1997) LLNL data base, still rely on the incoherent scattering function $S(x, Z)$ approach. For these compilations, the incoherent scattering cross section σ_{incoh} was obtained by numerical integration of the Klein–Nishina (1929) formula weighted by the incoherent scattering function $S(x, Z)$. The required values of $S(x, Z)$ were taken from the compilation by Hubbell *et al* (1975) for all Zs 1 to 100, with a span of x values sufficient for computing σ_{incoh} over the photon energy range 100 eV to 100 GeV, which were computed and tabulated in this compilation. Radiative and double-Compton corrections from Mork (1971) were applied to the integrated values for σ_{incoh}.

The Hubbell *et al* (1975) $S(x, Z)$ values were pieced together from data available in the literature, including the work of Pirenne (1946) ($Z = 1$), Brown (1970a, b, 1972, 1974) ($Z = 2$ to 6, with configuration interaction) and by Cromer and Mann (1967) and Cromer (1969) ($Z = 7$ to 100, from a non-relativistic Hartree–Fock model). Although giving cross sections differing by up to 2–3% from calculations of cross sections for isolated cases using relativistic S-matrix and other more sophisticated models, their compactness and ease of use makes these $S(x, Z)$ and σ_{incoh} values still (by default) the reference set used in most medical, biological and other practical applications. Some insight into the limitations and use of $S(x, Z)$ tables, and possible refinements, can be found in the treatments by Ribberfors and Berggren (1982) and by Namito *et al* (1994, 1995).

3.2.2. Coherent/Rayleigh/elastic scattering σ_{coh}. Rayleigh scattering is a process by which photons are scattered by bound electrons and in which the atom is neither ionized nor excited. The photon loses only a negligible fraction of its energy, since the recoil is by the entire atom including the nucleus, rather than by an individual atomic electron as in the Compton effect, and the scattering is 'coherent' resulting in interference effects. Since this scattering is peaked in the forward direction, particularly at high energies, this cross section has sometimes been neglected in photon transport computations. However, when this coherence is spread over an array of atoms, the interference becomes the Bragg diffraction which is of central importance in x-ray crystallography, crystal diffraction spectrometry and other areas including studies of molecular structures of biological interest.

The association of the name 'Rayleigh' with this process stems from researches on the scattering and polarization of visible light by gas molecules ('blue skies, red sunsets') by Strutt (Lord Rayleigh) (1871, 1881). A summary of this and other photon scattering work by Strutt (Lord Rayleigh) has been given in the more recent literature by Young (1982). This process is also sometimes called 'elastic' scattering, and this terminology is used in the extensive review by Kane *et al* (1986).

For compilations of μ/ρ in the medical and biological region of interest, the coherent scattering cross section σ_{coh} has been computed by numerical integration of the Thomson (1906) formula weighted by $F^2(x, Z)$, where $F(x, Z)$ is the atomic form factor. As in the somewhat complementary incoherent scattering function $S(x, Z)$, x is the momentum transfer variable dependent on the incident photon energy and the deflection angle of the scattered photon, and Z is the atomic (charge) number of the nucleus of the target atom.

Measured values of $F(x, Z)$ were compared graphically with theory in the review and compilation by Hubbell *et al* (1975). Although relativistic Hartree–Fock values were available at that time, the $F(x, Z)$ values tabulated for $7 \leqslant Z \leqslant 100$ were taken from the non-relativistic Hartree–Fock Cromer and Mann (1968) and Cromer (1971) results, in view of the approximate complementarity with $S(x, Z)$ then systematically available only from non-relativistic computations. For $Z = 1$ the $F(x, Z)$ values in Hubbell *et al* (1975) were

computed from the 'exact' formula of Pirenne (1946), and for $Z = 2$ to 6 were taken from the configuration interaction calculations by Brown (1970a, b, 1971, 1974). Thus, in the Hubbell *et al* (1975) compilation, both $S(x, Z)$ and $F(x, Z)$ are tabulated for all $Z = 1$ to 100 over the range $0.005\ \text{Å}^{-1} \leqslant x \leqslant 10^9\ \text{Å}^{-1}$, and both σ_{incoh} and σ_{coh} are tabulated for all $Z = 1$ to 100 over the photon energy range 100 eV to 100 MeV.

In the Berger–Hubbell (1987) XCOM μ/ρ data set, and in the Hubbell–Seltzer (1995) tabulation, the values of σ_{coh} are taken the relativistic compilation of Hubbell and Øverbø (1979). For these computations, relativistic theoretical values of $F(x, Z)$ were pieced together from Pirenne (1946) for $Z = 1$, and for the other elements, over the different ranges of x and Z, from Doyle and Turner (1968), Cromer and Waber (1974) and from Øverbø (1977a, 1978a). Somewhat higher accuracy is anticipated from the relativistic Hartree–Fock–Slater modified atomic form factor (MFF) calculations by Schaupp *et al* (1983) for $F(x, Z)$ for $Z = 1$ to 100, $0 \leqslant x \leqslant 100\ \text{Å}^{-1}$. This compilation was not accompanied by corresponding integrated values of σ_{coh}, and these MFF values have not yet found their way into the μ/ρ compilations for medical and biological applications.

Current theoretical efforts toward improved values of the coherent scattering cross section σ_{coh} are focused on use of the second-order relativistic S-matrix formalism (for example Kissel *et al* 1980, Pratt *et al* 1994, Kissel 1995). This formalism is capable of revealing anomalous scattering, particularly in the vicinity of absorption edge energies. For example, Zhou *et al* (1992) estimate that anomalous scattering effects can be as much as 15% at the absorption edge (subshell ionization threshold) energy, decreasing to less than 7% at 0.007 keV above the threshold, to less 5% at 0.045 keV above threshold, and to less than 3% for an incident photon energy 0.35 keV above the threshold. However, one loses the convenience and ease of application of the atomic form factor approach, although these details may be of more interest in the future.

3.3. Pair and triplet production, σ_{pair} (or κ_n) and σ_{trip} (or κ_e)

3.3.1. Electron–positron pair production. In this effect, which is the most likely photon interaction at high energies (above ~10 MeV), a photon disappears in the field of a charged particle, and an electron–positron pair appears. The cross section σ_{pair} for pair production in the field of the atomic nucleus varies approximately as the square of the nuclear charge Z, i.e.

$$\sigma_{\text{pair}} \propto \sim Z^2. \tag{8}$$

The cross section σ_{trip} (triplet) in the field of one of the atomic electrons varies as Z times the square of the unit charge, or

$$\sigma_{\text{trip}} \propto \sim Z. \tag{9}$$

This cross section is usually called the 'triplet' cross section, since the atomic electron involved in this process is also ejected from the atom, giving rise to a trident signature including the created electron and positron, when observed in a cloud chamber.

For $Z = 1$ (hydrogen) σ_{trip} is approximately equal to σ_{pair}, and it becomes progressively less important for higher Z materials, according to

$$\sigma_{\text{trip}}/\sigma_{\text{pair}} \approx 1/Z. \tag{10}$$

Since biological materials, except for bone, are primarily low Z, σ_{trip} can be a minor but significant contribution for high-energy photon applications (i.e. above ~10 MeV).

Both σ_{pair} and σ_{trip} are extensively reviewed, calculations are performed, and tabulations of these cross sections are provided for all elements $Z = 1$ to 100 over the photon energy range 1 MeV to 100 GeV in Hubbell *et al* (1980). Values from this 1980 publication are still

used in current μ/ρ compilations, for example Berger and Hubbell (1987) (XCOM), Hubbell and Seltzer (1995) and Cullen *et al* (1997). Some highlights of how these pair and triplet cross sections were calculated are given below.

3.3.2. Pair production cross section (coherent, in screened nuclear field), σ_{pair} (or κ_n). In coherent production, an electron–positron pair is produced in the screened nuclear field (i.e. atomic field), and the atom as a whole recoils without internal excitation. This is in contrast to incoherent (triplet) production $\sigma_{\rm trip}$ in which the atom is either excited or ionized and the target electron recoil significantly affects the dynamics and threshold of the process. In the case of $\sigma_{\rm pair}$, the threshold for this transmutation of electromagnetic energy (a photon) into tangible matter (electron and positron) is just the sum of the rest-mass energies ($m_{e^-} = m_{e^+} = 9.109\,3897 \times 10^{-28}$ g $= 0.510\,999\,06$ MeV (Cohen and Taylor 1986)) of the two particles, or 1.022 MeV.

The $\sigma_{\rm pair}$ calculation (Hubbell *et al* 1980) begins with the Bethe–Heitler (1934) Born approximation unscreened pair-production cross section as an initial approximation, to which Coulomb corrections, screening corrections and radiative corrections are applied. The differential Bethe–Heitler unscreened $\sigma_{\rm pair}$ cross section has been cast in forms suitable for computation by Bethe and Maximon (1954), Davies *et al* (1954) and Maximon (1968).

The Coulomb correction for the Hubbell *et al* (1980) computations was pieced together from the low-energy results of Øverbø *et al* (1968, 1973), the intermediate-energy results of Øverbø (1977b) and the high-energy results of Sørenssen (1965, 1966) which in the high-energy limit go to the Davies *et al* (1954) extreme relativistic Coulomb correction. Screening corrections were pieced together from the near-threshold results of Tseng and Pratt (1972, 1980) and the intermediate- and high-energy work of Øverbø (1978b). The Øverbø (1978b) work used the Jost *et al* (1950) expression for nuclear-field pair production in the Born approximation for small nuclear recoil but without the extreme high-energy approximation. This expression required values of the atomic form factor $F(x, Z)$, for which Øverbø (1978b) used the relativistic $F(x, Z)$ values pieced together from Doyle and Turner (1968), Cromer and Waber (1974) and Øverbø (1977a, 1978a), later published as systematic tabulations by Hubbell and Øverbø (1979). The radiative corrections (Feynman 1949, Mork and Olsen 1960), of the order of 1/137 and associated with the emission and reabsorption of virtual photons and with the emission of both soft and hard real photons, were obtained from Mork and Olsen (1965).

3.3.3. Triplet production cross section (incoherent pair production, in electron field, with excitation or ionization), σ_{trip} (or κ_e). Due to the sharing of photon energy and momentum between the target electron and the created pair, the threshold for this process is $4m_ec^2 (= 2.044$ MeV). Actually, the process can take place down to $2m_ec^2$, since momentum can also be transferred to the atom both in excitation and ionization, but in this region the cross section is negligibly small. Some of the highlights of the calculations and systematic tabulations of $\sigma_{\rm trip}$ by Hubbell *et al* (1980), as a companion to the $\sigma_{\rm pair}$ tabulations therein, are given in the following.

The starting point for these computations of $\sigma_{\rm trip}$ is again the Bethe–Heitler (1934) Born approximation, now requiring the retardation effect due to the recoil of the target atomic electron. This effect is included in the unscreened formula of Borsellino (1947), improved by including higher terms by Ghizzetti (1947). Corrections for exchange could be obtained as a ratio of results by Haug (1975) to the Borsellino–Ghizzetti results which neglected this

effect. A scheme for including screening is given by Wheeler and Lamb (1939) who presented some results computed using Thomas–Fermi (Thomas 1927, Fermi 1928) statistical-atomic-model values of $S(x, Z)$. In the Hubbell *et al* (1980) computations, screening corrections were obtained by replacing the Thomas–Fermi $S(x, Z)$ values in the Wheeler–Lamb formula by the $S(x, Z)$ values in Hubbell *et al* (1975) based on the configuration-interaction $Z = 2$ to 6 values of Brown (1970a, b, 1972, 1974) and non-relativistic Hartree–Fock $Z = 7$ to 100 values of Cromer and Mann (1967) and Cromer (1969).

4. The mass energy-absorption coefficient μ_{en}/ρ

A companion coefficient to μ/ρ of particular interest in medical and biological applications is the mass energy-absorption coefficient μ_{en}/ρ, used for computing the energy deposition (ionization, excitation, heat, etc) at a site (a 'volume of interest') within a mass of irradiated target material. For detailed discussions and the mathematical expressions for computing this coefficient, the reader is referred particularly to the definitive work of Berger (1961), also to the work of Hubbell (1982) widely used as a reference standard, and to the more recent works of Seltzer (1993) and Hubbell and Seltzer (1995).

Here, μ_{en}/ρ will be defined pictorially in figure 4 (from Hubbell 1977, which is also the source of the following text)), in terms of the progressively more-detailed quantities μ/ρ, μ_a/ρ, μ_{tr}/ρ and μ_{en}/ρ, reading from left to right across the bottom of the diagram. Each of the photon interaction cross sections appearing in the sum on the right-hand side of equation (6) is represented schematically on the vertical left-hand side of figure 4 as the base dimension of a broad arrow. Moving from left to right along each of these arrows representing an interaction process, upward-branching arrows have been drawn to represent the fraction of the initial photon energy lost to the volume of interest in the form of secondary photons.

These secondary photons can include not only scattered and fluorescence photons from the primary event, but also bremsstrahlung and annihilation radiation from the charged-particle products of the primary event. The remaining fractional photon energy is assumed to be available for deposit in the volume of interest via the various charged-particle energy-dissipation mechanisms (see, for example, Seltzer 1993). For application to absorbed-dose calculations, information on this available energy can be represented by the various approximate coefficients μ_a/ρ, μ_{tr}/ρ and μ_{en}/ρ listed across the bottom of figure 4. Each of these coefficients has the same dimensions (for example $cm^2\ g^{-1}$) as the mass attenuation coefficient μ/ρ but is reduced by a fraction which takes into account a specified combination of secondary photon energy losses as schematically indicated by the connecting broken lines in figure 4.

4.1. The mass absorption coefficient μ_a/ρ

The simplest of these approximate coefficients, μ_a/ρ, referred to by Evans (1955, 1968) as the 'mass absorption coefficient', assumes, as indicated in figure 4, that only scattered photons, both coherent and incoherent, leave the volume of interest. Usually included in this approximation is the assumption that incoherent (Compton) scattering is adequately described by the Klein–Nishina (1929) equations which assume the target electrons to be initially free and at rest.

4.2. The mass energy-transfer coefficient μ_{tr}/ρ

The next approximation, discussed in ICRU Report 33 (ICRU 1980), is the 'mass energy-transfer coefficient' μ_{tr}/ρ symbolized by the broken line in figure 4 connecting to this quantity.

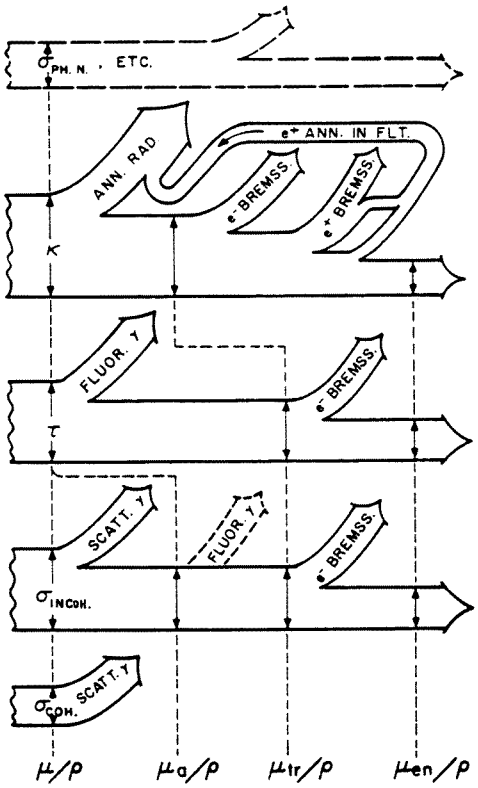

Figure 4. Schematic representation of the mass attenuation coefficient μ/ρ, the mass absorption coefficient μ_a/ρ, the mass energy-transfer coefficient $\mu_{\rm tr}/\rho$, and the mass energy-absorption coefficient $\mu_{\rm en}/\rho$ in terms of the cross sections for coherent ($\sigma_{\rm COH}$) and incoherent ($\sigma_{\rm INCOH}$) scattering, atomic photoeffect (τ), pair production (κ), and photonuclear reactions ($\sigma_{\rm PH.N.}$). The upward-branching arrows represent the fraction, of the incident photon energy, lost to the volume of interest in the form of secondary photons such as positron annihilation radiation (ANN. RAD.), bremsstrahlung (e^-, e^+ BREMSS.), fluorescence x-rays (FLUOR. γ) and scattered photons (SCATT. γ). The enhancement of annihilation photon energies due to positron annihilation in flight (e^+ ANN. IN FLT.) at the expense of positron bremsstrahlung and energy deposition is also indicated.

This coefficient assumes that *all* secondary photons from the primary event, fluorescence as well as scattered photons, are lost to the volume of interest. In addition, although born subsequent to the primary interaction at a distance determined by the positron travel prior to annihilation, annihilation radiation (two 0.511 MeV photons, here assuming annihilation to take place only after the positron has come to rest) is included in the fractional energy subtractions in computing $\mu_{\rm tr}/\rho$.

4.3. The mass energy-absorption coefficient μ_{en}/ρ

The further-reduced 'mass energy-absorption coefficient' $\mu_{\rm en}/\rho$ indicated symbolically as the broken line at the extreme right edge of figure 4, is still a somewhat inexact quantity due to the arbitrariness of the 'volume of interest' and other factors, but is an improvement over the above

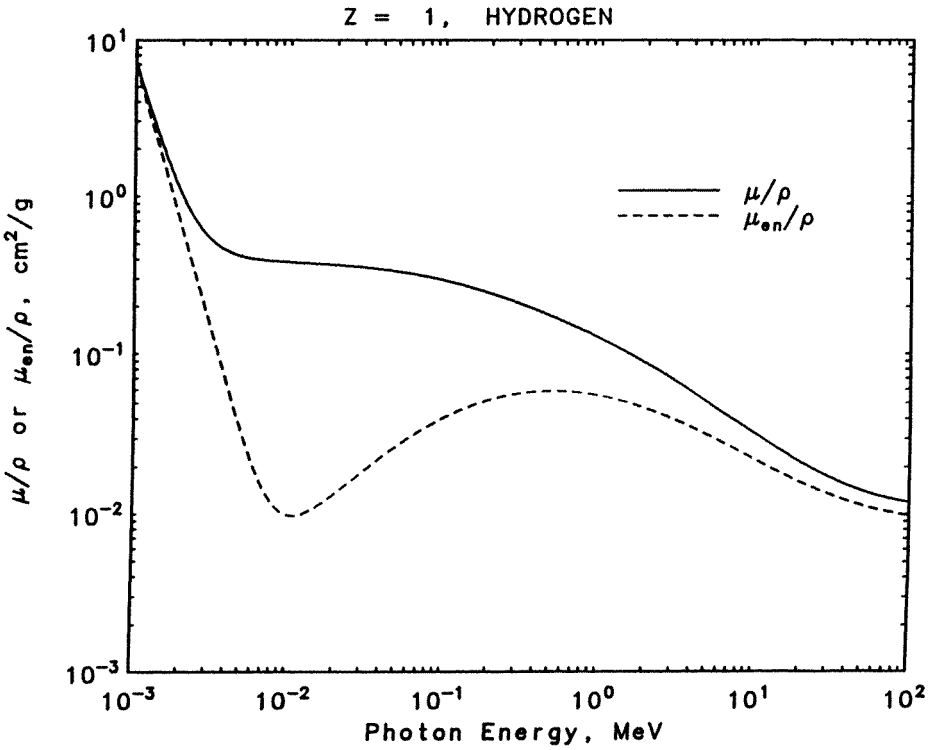

Figure 5. The mass attenuation coefficient μ/ρ and mass energy absorption coefficient μ_{en}/ρ for hydrogen for photon energies 1 keV to 100 MeV.

coefficients if one is to use this general approach in computing energy deposition. Seltzer's (1993) calculations address all the criticisms by Carlsson (1971) of earlier μ_{en}/ρ computations, by taking into account (i) electron binding effects on the Compton-scattered photon distribution, (ii) the complete cascade of fluorescence emission after ionization events in any atomic subshell, including those associated with incoherent scattering and triplet production, and (iii) the radiative energy losses of the secondary electrons and positrons slowing down in the medium, including the emission of bremsstrahlung, characteristic x-rays from impact ionization, and positron in-flight as well as at-rest annihilation quanta. His consideration of the processes in (iii) goes beyond the continuous-slowing-down approximation and includes the effects of energy-loss straggling.

Figures 5, 6 and 7 from Hubbell and Seltzer (1995) show some sample results for μ_{en}/ρ for H ($Z = 1$), water and Cu ($Z = 29$), compared with μ/ρ taken from the Berger–Hubbell (1987) XCOM PC data base. It is clear that for low-Z materials, in which incoherent scattering is the dominant process in the energy range of interest in medicine and biology, the fraction of photon energy deposited in the medium is small, but increases for higher-Z materials where photoelectric absorption is more significant. For compounds and mixtures, it should be pointed out that μ_{en}/ρ values cannot be simply added together according to fractions by weight, as in the case of μ/ρ, due to the matrix effect (secondary radiations produced by atoms differing from the original target atom) on the calculation.

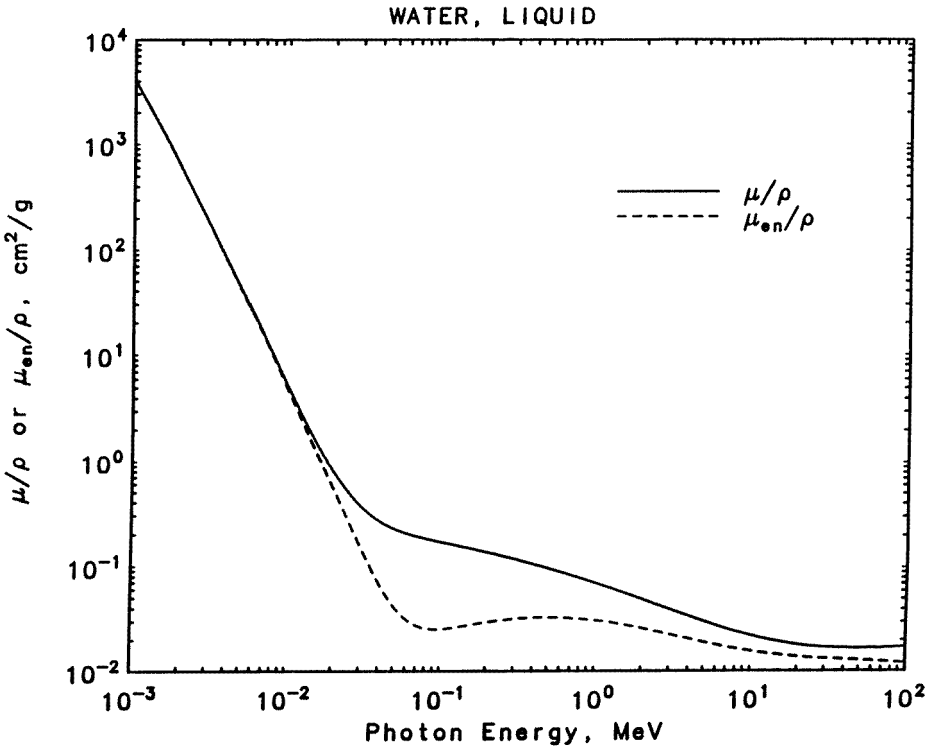

Figure 6. The mass attenuation coefficient μ/ρ and mass energy absorption coefficient μ_{en}/ρ for water for photon energies 1 keV to 100 MeV.

5. Current status and future tasks, particularly for medical and biological applications

It is clear from the above account that the μ/ρ tables used in medical, biological and other applications are indebted to a great army of theoretical physicists, working on the many pieces of the puzzle, from the time of Röntgen (1895) to the present. These tables are further indebted to the even greater army of experimental physicists listed in the Hubbell (1994) bibliography whose results the theory must reproduce at the points where comparison is possible. If such reproduction is achieved, within the uncertainties of the theoretical models and the experimental measurements, then we feel we have some understanding of the underlying reality of the physical entities and processes involved in the interactions of the photons with tangible matter.

Many of the above calculations and computations, still used in current μ/ρ compilations, were performed on rather rudimentary computers, compared with what are available today. Hence, new computations are anticipated, to replace the old, using newer approaches such as the relativistic S-matrix formalism. One would hope that the value of μ/ρ obtained from improved measurements and better theoretical models, for any given combination of Z and incident photon energy, is converging in time asymptotically, as the years pass, to an 'underlying reality' μ/ρ, although there have been some notable divergences in the past. Hence it has been difficult to establish an 'envelope of uncertainty' as desired by workers in radiation dosimetry reference standards.

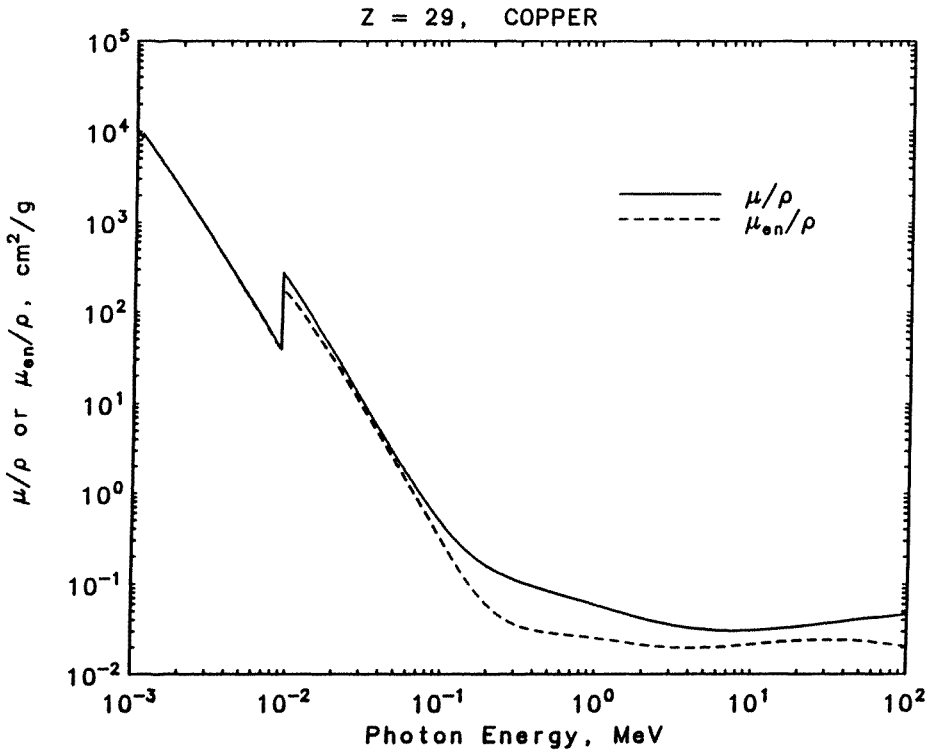

Figure 7. The mass attenuation coefficient μ/ρ and mass energy absorption coefficient μ_{en}/ρ for copper for photon energies 1 keV to 100 MeV.

Table 1. EPDL97 photoionization cross section estimated uncertainties (1σ assumed).

Photon energy range	Solid	Gas
1 eV–10 eV	?	?
10 eV–100 eV	1000%	20%
100 eV–0.5 keV	100%–200%	10%–20%
0.5 keV–1.0 keV	10%–20%	5%
1.0 keV–5.0 keV	5%	5%
5 keV–100 keV	2%	2%
100 keV–10 MeV	1%–2%	1%–2%
10 MeV–100 GeV	2%–5%	2%–5%

For the photoionization cross section, an attempt has been made in EPDL97 (Cullen *et al* 1997) to provide some rough estimates of the envelope of uncertainty, over the ranges of photon energies encompassed in that data base (table 1). Since photoionization or atomic photoeffect is the dominant interaction at low photon energies, where the uncertainties are the largest, these very approximate and subjective percent uncertainties can be taken as a rough guide to the uncertainties of the total photon cross section σ_{tot} or the mass attenuation coefficient μ/ρ. In the region 5 MeV to 30 MeV where the photonuclear giant dipole resonance occurs in the photonuclear cross section $\sigma_{ph.n.}$, neglect of this cross section can make errors in μ/ρ in excess of 5%, at the peak of this resonance. This $\sigma_{ph.n.}$ peak energy varies with both Z and the particular isotope of that element.

From this we can see that in the photon energy range of most interest in medical and biology applications, 5 keV to a few MeV, the envelope of uncertainty of μ/ρ, judging from the above estimates, is of the order of 1% to 2%. For the photon energy range 1 keV to 50 MeV, of most interest to medical physicists, attention is here called to a recently assembled electronic data base, including values of $\mu_{\rm en}/\rho$, developed by Boone and Chavez (1996).

Some notion of the convergence of μ/ρ as a function of time may be had by selecting a photon energy, here 40 keV, and two elements, here carbon and lead, and following the variations in these μ/ρ values from the first compilation to use a standard energy grid (White 1952), through to the values given by Hubbell and Seltzer (1995) and by Boone and Chavez (1996) (table 2).

Table 2. Variance of compiled values of μ/ρ as a function of time.

	μ/ρ (cm^2 g^{-1}) ('with coherent')	
Compilation (at 40 keV)	C ($Z = 6$)	Pb ($Z = 82$)
White (1952)	0.202	10.5
White Grodstein (1957)	0.205	10.5
McGinnies (1959)	0.205	15.1
Allison (1961)	—	14.3
Brown (1966)	0.193	14.3
Plechaty and Terrall (1966)	0.208	13.2
Hubbell (1969)	0.206	14.0
McMaster *et al* (1969)	0.205	14.1
Johns and Cunningham (1969)	0.205	13.8
Storm and Israel (1970)	0.207	14.2
Veigele (1973)	0.209	14.2
Hubbell (1982)	0.207	14.4
Hubbell and Seltzer (1995)	0.208	14.4
Boone and Chavez (1996)	0.207	14.3

The stability of the μ/ρ values beginning in the 1960s, particularly for Pb for which 40 keV is below the K-shell photoabsorption edge (only L and higher shells contributing) can be attributed to a combination of the higher-shell photoeffect cross section calculations by Rakavy and Ron (1965, 1967) and by Scofield (1973), with a flurry of new measurements in this time period.

For future tasks, more attention should be paid to the atomic photoeffect absorption edge structure, which will require a much larger and higher-dimensional data base, to accommodate the molecular and other matrix environments of the target atoms. Similarly, for the more accurate scattering results from the relativistic S-matrix theoretical model, to replace the current simplistic and approximate $F(x, Z)$ and $S(x, Z)$ atomic form factor and incoherent scattering function tables, much more extensive and higher-dimensional arrays will be required. However, modern computers continue to take giant steps toward greater computing power, speed and data storage and retrieval, so these objectives should be met within the coming decade, perhaps even including photonuclear data $\sigma_{\rm ph.n.}$.

At the same time, the experimental capabilities, including more intense and higher-energy synchrotron light sources, and new detectors with better resolution and higher efficiencies, should provide more accurate (toward 'underlying reality'?) measured values of μ/ρ to test and undergird the above theoretical advances. Although it is sometimes said that 'now theory is better than experiment', the belief of this author is that 'theory is an interpolation of experiment' for purposes of compiling μ/ρ tables for medical, biological and other practical applications.

References

Allen S J M 1924 The absorption coefficients of homogeneous x-rays between wave-lengths 0.1 and 0.71 Å *Phys. Rev.* **24** 1–8

——1926 The absorption of x-rays of wave-length down to 0.08 Å *Phys. Rev.* **26** 266–76

——1935 Mean values of the mass absorption coefficients of the elements *X-Rays in Theory and Experiment* ed A H Compton and S K Allison (New York: Van Nostrand) Appendix IX, pp 799–806

——1971/1972 Mass absorption coefficients for x and γ-rays *Handbook of Chemistry and Physics* ed R C Weast (Cleveland, OH: CRC Press) pp E-123–E-124

Alling W R and Johnson W R 1965 Exact calculations of K-shell and L-shell photoeffect *Phys. Rev.* **139** A1050–A1062

Allison J W 1961 Gamma-radiation absorption coefficients of various materials allowing for bremsstrahlung and other secondary radiations *Aust. J. Phys.* **14** 443–68

Azároff L V 1963 Theory of extended fine structure of x-ray absorption edges *Rev. Mod. Phys.* **35** 1012–22

Barkla C G and Sadler C A 1907 Secondary x-rays and the atomic weight of nickel *Phil. Mag.* **14** 408–22

——1909 The absorption of Röntgen rays *Phil. Mag.* **17** 739–60

Beer A 1852 Bestimmung der Absorption des roten Lichts in farbingen Flüssigkeiten *Ann. Phys., Lpz.* **86** 78–88

Berger M J and Hubbell J H 1987 XCOM: photon cross sections on a personal computer *NBSIR* 87-3597 (Washington, DC: NBS)

——1998/1999 Photon attenuation coefficients *CRC Handbook of Chemistry and Physics* 79th edn, ed D R Lide (Boca Raton, FL: CRC Press) pp 10-207–10-211

Berger R T 1961 The x- or gamma-ray energy absorption or transfer coefficient: tabulations and discussion *Radiat. Res.* **15** 1–29

Bergstrom P M and Pratt R H 1997 An overview of the theories used in Compton scattering calculations *Radiat. Phys. Chem.* **50** 3–29

Bergstrom P M, Surić T, Pisk K and Pratt R H 1992 Some preliminary calculations of whole atom Compton scattering af unpolarized photons *Nucl. Instrum. Methods* B **71** 1–6

——1993 Compton scattering of photons from bound electrons: full relativistic independent-particle-approximation calculations *Phys. Rev.* A **48** 1134–62

Bethe H A and Heitler W 1934 On the stopping of fast particles and on the creation of positive electrons *Proc. R. Soc.* A **146** 83–112

Bethe H A and Maximon L C 1954 Theory of bremsstrahlung and pair production. I. Differential cross section *Phys. Rev.* **93** 768–84

Biggs F and Lighthill R 1971 Analytical approximations for x-ray cross sections. II *Sandia Laboratories Report* SC-RR-71-0507

Boone J M and Chavez A E 1996 Comparison of x-ray cross sections for diagnostic and therapeutic medical physics *Med. Phys.* **23** 1997–2005

Borsellino A 1947 Sulle coppie di elettroni create da raggi γ in presenza di elettroni *Nuovo Cimento* **4** 112–30

Bouguer P 1729 *Essai d'Optique sur la Gradation de la Lumière* (Havre, France)

Bradley D A (ed) 1997 Inelastic scattering of x-rays and gamma rays *Radiat. Phys. Chem.* **50** (1) (special issue)

Brown R T 1970a Coherent and incoherent x-ray scattering by bound electrons. I. Helium isoelectronic sequence *Phys. Rev.* A **1** 1342–7

——1970b Coherent and incoherent x-ray scattering by bound electrons II. Three- and four-electron atoms *Phys. Rev.* A **2** 614–20

——1971 Atomic form factor for neutral carbon *J. Chem. Phys.* **55** 353–5

——1972 Incoherent-scattering function for atomic carbon *Phys. Rev.* A **5** 2141–4

——1974 Coherent and incoherent x-ray scattering by bound electrons. III. Five-electron atoms *Phys. Rev.* A **10** 438–9

Brown W D 1966 X-ray attenuation and absorption coefficients *Boeing Report* D2-125065-1

Carlsson G A 1971 A criticism of existing tabulations of mass energy transfer and mass energy absorption coefficients *Health Phys.* **20** 653–4

Chantler C T 1995 Theoretical form factor, attenuation and scattering tabulation for $Z = 1$–92 from $E = 1$–10 eV to $E = 0.4$–1.0 MeV *J. Phys. Chem. Ref. Data* **24** 71–643

Cohen E R and Taylor B N 1986 The 1986 adjustment of the fundamental constants *CODATA Bulletin 63* (values republished most recently in *Physics Today* August 1997, BG7-BG11)

Cooper M J 1997 Compton scattering and the study of electron momentum density distributions *Radiat. Phys. Chem.* **50** 63–76

Creagh D C and Hubbell J H 1987 Problems associated with the measurement of x-ray attenuation coefficients. I. Silicon. Report on the International Union of Crystallography x-ray attenuation project *Acta Crystallogr.* A **43** 102–12

Creagh D C and Hubbell J H 1987 1990 Problems associated with the measurement of x-ray attenuation coefficients. II. Carbon. Report on the International Union of Crystallography x-ray attenuation project *Acta Crystallogr.* A **46** 402–8

——1992 X-ray absorption (or attenuation) coefficients *International Tables for Crystallography* vol C, ed A J C Wilson (Dordrecht: Kluwer) pp 189–206

Cromer D T 1969 Compton scattering factors for aspherical free atoms *J. Chem. Phys.* **50** 4857–9

——1971 *Private communication* to W J Veigele and J H Hubbell

Cromer D T and Mann J B 1967 Compton scattering factors for spherically symmetric free atoms *J. Chem. Phys.* **47** 1892–983

——1968 X-ray scattering factors computed from numerical Hartree–Fock wave functions *Acta Crystallogr.* A **24** 321–4

Cromer D T and Waber J T 1974 Atomic scattering factors for x-rays *International Tables for X-Ray Crystallography* vol 4 (Birmingham: Kynoch) pp 71–147

Cullen D E, Chen M H, Hubbell J H, Perkins S T, Plechaty E F, Rathkopf J A and Scofield J H 1989 Tables and graphs of photon-interaction cross sections from 10 eV to 100 GeV derived from the LLNL evaluated photon data library (EPDL), Part A: $Z = 1$ to 50; Part B: $Z = 51$ to 100 *Lawrence Livermore National Laboratory Report* UCRL-50400, vol 6, rev 4

Cullen D E, Hubbell J H and Kissel L 1997 EPDL97: The evaluated photon data library *Lawrence Livermore National Laboratory Report* UCRL-50400, vol 6, rev 5

Davies H, Bethe H A and Maximon L C 1954 Theory of bremsstrahlung and pair production. II. Integral cross section for pair production *Phys. Rev.* **93** 788–95

Davisson C M 1955 Interaction of γ-radiation with matter and γ-ray absorption coefficients *Beta- and Gamma-Ray Spectroscopy* ed K Siegbahn (Amsterdam: North-Holland) pp 24–51, 857–74

——1965 Interaction of γ-radiation with matter and γ-ray attenuation coefficients *Alpha-, Beta- and Gamma-Ray Spectroscopy* ed K Siegbahn (Amsterdam: North-Holland) pp 37–78, 827–43

Davisson C M and Evans R D 1952 Gamma-ray absorption coefficients *Rev. Mod. Phys.* **24** 79–107

Del Grande N K 1986 Measured 1 to 40 keV photoabsorption cross sections for: Fe, Ni, Sn, Ta, Pt, Au, Pb, U *Proc. SPIE* **691** 2–10

——1990 L shell photoabsorption spectroscopy for solid metals: Ti, V, Cr, Fe, Ni, Cu *Phys. Scr.* **41** 110–14

Deslattes R D 1969 Estimates of x-ray attenuation coefficients for the elements and their compounds *Acta Crystallogr.* A **25** 89–93

Dietrich S S and Berman B L 1988 Atlas of photoneutron cross sections obtained with monoenergetic photons *At. Data Nucl. Data Tables* **38** 199–338

Doyle P A and Turner P S 1968 Relativistic Hartree–Fock x-ray and electron scattering factors *Acta Crystallogr.* A **24** 390–7

Evans R D 1955 *The Atomic Nucleus* (New York: McGraw-Hill) p 711

——1968 X-ray and γ-ray interactions *Radiation Dosimetry* vol 1, ed F H Attix and W C Roesch (New York: Academic) pp 93–155

Faessler A 1955 Röntgenspektrum und Bindungszustand *Landolt-Börnstein Zahlenwerte und Funktionen aus Physik, Chemie, Astronomie, Geophysik und Technik* ed A Eucken (Berlin: Springer) pp 769–868

Fano U 1953 Gamma-ray attenuation. Part I. Basic processes *Nucleonics* **11** 8–12; Part II. Analysis of penetration *Nucleonics* **11** 55–61

Fermi E 1928 Eine statistiche Methode zur Bestimmung einiger Eigenschaften des Atomes und ihre Anwendung auf die Theorie des periodischen Systems der Elemente *Z. Phys.* **48** 73–9

Feynman R P 1949 The theory of positrons *Phys. Rev.* **76** 749–59

Fuller E G and Hayward E 1976 *Photonuclear Reactions* (Strondsburg, PA: Dowden, Hutchinson & Ross)

Gerward L 1993 X-ray attenuation coefficients: current state of knowledge availability *Radiat. Phys. Chem.* **41** 783–9

Ghizzetti A 1947 Teoria della produzione di coppie di elettroni *Rev. Math. Fis. Teor. Tucuman (Ser. A)* **6** 37–50

Gimm H A and Hubbell J H 1978 Total photon absorption cross section measurements, theoretical analysis and evaluations for energies above 10 MeV *NBS Technical Note* 968

Harding G 1997 Inelastic scattering effects and applications in biomedical science and industry *Radiat. Phys. Chem.* **50** 91–111

Haug E 1975 Bremsstrahlung and pair production in the field of free electrons *Z. Naturforsch.* **30a** 1099–113

Hayward E 1970 Photonuclear reactions *NBS Monograph* 118

Heinrich K F J 1966 X-ray absorption uncertainty *The Electron Microprobe* ed T D McKinley, K F J Heinrich and D B Wittry (New York: Wiley) pp 296–377

——1986 Mass absorption coefficients for electron probe microanalysis *Proc. 11th Int. Congress on X-Ray Optics and Microanalysis (London, Ontario)* ed J D Brown and R H Packwood, pp 67–119

Henke B L, Elgin R L, Lent R E and Ledingham R B 1967 X-ray absorption in the 2-to-200 Å region *Norelco Rep.* **14** 112–31

Henke B L, Gullikson E M and Davis J C 1993 X-ray interactions: photoabsorption, scattering, transmission and reflection at $E = 50$–30,000 eV, $Z = 1$–92 *At. Data Nucl. Data Tables* **54** 181–342

Henke B L, Lee P, Tanaka T J, Shimabukuro R L and Fujikawa B K 1982 Low-energy x-ray interaction coefficients: photoabsorption, scattering, and reflection, $E = 100$–2000 eV $Z = 1$–94 *At. Data Nucl. Data Tables* **27** 1–144

Hubbell J H 1953 Attenuation coefficients extrapolated to zero absorber thickness (unpublished)

——1969 Photon cross sections, attenuation coefficients, and energy absorption coefficients from 10 keV to 100 GeV *NSRDS-NBS* 29

——1971 Survey of photon-attenuation-coefficient measurements 10 eV to 100 GeV *At. Data* **3** 241–97

——1977 Photon mass attenuation and mass energy-absorption coefficients for H, C, N, O, Ar, and seven mixtures from 0.1 keV to 20 MeV *Radiat. Res.* **70** 58–81

——1982 Photon mass attenuation coefficients and energy-absorption coefficients from 1 keV to 20 MeV *Int. J. Appl. Radiat. Isot.* **33** 1269–90

——1994 Bibliography of photon total cross section (attenuation coefficient) measurements 10 eV to 13.5 GeV, 1907–1993 *NISTIR* 5437

——1996 Experimentally measured total x-ray attenuation coefficients extracted from previously unprocessed documents held by the NIST photon and charged particle data center *NISTIR* 5893

——1997 Summary of existing information on the incoherent scattering of photons, particularly on the validity of the use of the incoherent scattering function *Radiat. Phys. Chem.* **50** 113–24

Hubbell J H and Berger M J 1968 Sec. 4.1: Attenuation coefficients, energy absorption coefficients, and related quantities, and sec. 4.2: Photon atomic cross sections *Engineering Compendium on Radiation Shielding* vol 1, ed R G Jaeger (Berlin: Springer) pp 167–202

Hubbell J H, Gerstenberg H M and Saloman E B 1986 Bibliography of photon total cross section (attenuation coefficient) measurements 10 eV to 13.5 GeV *NBSIR* 86-3461

Hubbell J H, Gimm H A and Øverbø I 1980 Pair, triplet, and total atomic cross sections (and mass attenuation coefficients) for 1 MeV–100 GeV photons in elements $Z = 1$ to 100 *J. Phys. Chem. Ref. Data* **9** 1023–147

Hubbell J H, McMaster W H, Del Grande N K and Mallett J H 1974 X-ray cross sections and attenuation coefficients *International Tables for X-Ray Crystallography* vol 4, ed J A Ibers and W C Hamilton (Birmingham: Kynoch) pp 47–70

Hubbell J H and Øverbø I 1979 Relativistic atomic form factors and photon coherent scattering cross sections *J. Phys. Chem. Ref. Data* **8** 69–105

Hubbell J H and Seltzer S M 1995 Tables of x-ray mass attenuation coefficients and mass energy-absorption coefficients 1 keV to 20 MeV for elements $Z = 1$ to 92 and 48 additional substances of dosimetric interest *NISTIR* 5632

Hubbell J H, Veigele Wm J, Briggs E A, Brown R T, Cromer D T and Howerton R J 1975 Atomic form factors, incoherent scattering functions, and photon scattering cross sections *J. Phys. Chem. Ref. Data* **4** 471–538 (erratum **6** 615–16 (1977))

Hultberg S, Nagel B and Olsson P 1961 Relativistic differential and total K-shell photoelectric cross-sections and photoelectron polarizations *Ark. Fys.* **20** 555–7

——1968 Numerical calculation of K-shell photoeffect *Ark. Fys.* **38** 1–96

ICRU 1980 Radiation quantities and units *ICRU Report* 33 (Bethesda, MD: ICRU)

Johns H E and Cunningham J R 1969 *The Physics of Radiology* 3rd edn (Springfield, IL: Thomas) (4th edn 1983)

Jost R, Luttinger J M and Slotnick M 1950 Distribution of recoil nucleus in pair production by photons *Phys. Rev.* **50** 189–96

Kane P P 1992 Inelastic scattering of x-rays and gamma-rays by inner shell electrons *Phys. Rep.* **218** 68–139

——1997 Experimental studies of inelastic x-ray and γ-ray scattering *Radiat. Phys. Chem.* **50** 31–62

Kane P P, Kissel L, Pratt R H and Roy S C 1986 Elastic scattering of γ-rays and x-rays by atoms *Phys. Rep.* **140** 75–159

Kissel L 1995 Toward improved photon-atom scattering predictions *Nucl. Instrum. Methods* B **99** 144–7

Kissel L, Pratt R H and Roy S C 1980 Rayleigh scattering by neutral atoms, 100 eV to 10 MeV *Phys. Rev.* A **22** 1970–2004

Klein O and Nishina Y 1929 Über die Streuung von Strahlung durch freie Elektronen nach der neuen relativistischen Quantendynamik von Dirac *Z. Phys.* **52** 853–68

Lambert J H 1760 *Photometria sive de Mensura et Gradibus Luminis Colorum et Umbrae* (Augsburg, Germany)

Leroux J 1960 Method for finding mass-absorption coefficients by empirical equations and graphs *Adv. X-Ray Anal.* **5** 153–60

Leroux J and Thinh 1977 *Revised Tables of X-Ray Mass Attenuation Coefficients* (Quebec: Corporation Scientifique Claisse)

Liebhafsky H A, Pfeiffer H G, Winslow E H and Zemany P D 1960 Appendix IV: values of the mass absorption coefficients of the elements in the region from 0.1 to 10 Å *X-Ray Absorption and Emission in Analytical Chemistry* pp 313–17

Lytle F W, Sayers D E and Stern E A 1975 Extended x-ray-absorption fine-structure technique. II. Experimental practice and selected results *Phys. Rev.* B **11** 4825–35

Manninen S 1997 Resonant Raman scattering and fluorescence spectroscopy *Radiat. Phys. Chem.* **50** 77–89

Martin R L 1988 Atomic weights of the elements 1987 *Pure Appl. Chem.* **60** 841–54

Matese J J and Johnson W R 1965 Influence of screening on the atomic photoeffect *Phys. Rev.* **140** A1–A7

Maximon L C 1968 Simple analytic expressions for the total Born approximation cross section for pair production in a Coulomb field *J. Res. Nat. Bur. Standards* B **72** 79–88

Maximon L C and Gimm H A 1981 Pair production in the field of atomic electrons *Phys. Rev.* A **23** 172–85

McGinnies R T 1959 X-ray attenuation coefficients from 10 keV to 100 MeV *NBS Suppl. to Circular* **583**

McMaster W H, Del Grande N K, Mallett J H and Hubbell J H 1969, 1970 Compilation of x-ray cross sections *Lawrence Livermore National Laboratory Report* UCRL-50174 (section I 1970, section II 1969, section III 1969, section IV 1969)

Mork K J 1971 Radiative corrections. II. Compton effect *Phys. Rev.* A **4** 917–27

Mork K and Olsen H 1960 Radiative corrections to pair production at high energies *Nuovo Cimento* **18** 395–6

——1965 Radiative corrections. I. High-energy bremsstrahlung and pair production *Phys. Rev.* B **140** 1661–74; erratum 1968 *Phys. Rev.* B **166** 1862

Namito Y, Ban S and Hirayama H 1994 Implementation of the Doppler broadening of a Compton-scattered photon into the EGS4 code *Nucl. Instrum. Methods* A **349** 489–94

Namito Y, Ban S, Hirayama H, Nariyama N, Nakashima H, Nakane Y, Sakamoto Y, Asano Y and Tanaka S 1995 Compton scattering of 20- to 40-keV photons *Phys. Rev.* A **51** 3036–43

Øverbø I 1977a Atomic form factors for large momentum transfers *Nuovo Cimento* B **40** 330–8

——1977b The Coulomb correction to electron pair production by intermediate-energy photons *Phys. Lett.* **71B** 412–14

——1978a Large-q form factors for light atoms *Phys. Scr.* **17** 547–8

——1978b Pair production by photons. Screening corrections for intermediate and high energies *Nuovo Cimento* A **47** 43–58

Øverbø I, Mork K J and Olsen H A 1968 Exact calculation of pair production *Phys. Rev.* **175** 1978–81

——1973 Pair production by photons: exact calculation for unscreened atomic field *Phys. Rev.* A **8** 668–85

Pirenne M H 1946 *The Diffraction of X-Rays and Electrons by Free Molecules* (London: Cambridge University Press) pp 12–28

Plechaty E F and Terrall J R 1966 Photon cross sections 1.0 keV to 15.0 MeV *Lawrence Radiation Laboratory Report* UCRL-50178

Pratt R H 1960 Atomic photoelectric effect at high energies *Phys. Rev.* **117** 1017–28

Pratt R H, Kissel L and Bergstrom P M 1994 New relativistic S-matrix results for scattering—beyond the usual anomalous factors/beyond impulse approximation *Resonant Anomalous X-Ray Scattering: Theory and Applications* ed G Materlik, C J Sparks and K Fischer (Amsterdam: Elsevier) pp 9–33

Pratt R H, Levee R D, Pexton R L and Aron W 1964 K-shell photoelectric cross sections from 200 keV to 2 MeV *Phys. Rev.* **134** A898–A915

Rakavy G and Ron A 1965 Total cross sections of the photoelectric effect for uranium *Phys. Lett.* **19** 207–8

——1967 Atomic photoeffect in the range $E_\gamma = 1$–2000 keV *Phys. Rev.* **159** 50–6

Ribberfors R and Berggren K-F 1982 Incoherent-x-ray-scattering functions and cross sections $(\mathrm{d}\sigma/\mathrm{d}\Omega')_{\mathrm{incoh}}$ by means of a pocket calculator *Phys. Rev.* A **26** 3325–33

Röntgen W C 1895 Über eine neue Art von Strahlen *Sitzungsber. Würzburger Phys.-Med. Gesellsch.* (reprinted in *Ann. Phys. Chem.* **64** 1 (1898))

Saloman E B and Hubbell J H 1986 X-ray attenuation coefficients (total cross sections): comparison of the experimental data base with the recommended values of Henke and the theoretical values of Scofield for energies between 0.1–100 keV *NBSIR* 86-3431 (Washington, DC: NBS)

Saloman E B, Hubbell J H and Scofield J H 1988 X-ray attenuation cross sections for energies 100 eV to 100 keV and elements $Z = 1$ to $Z = 92$ *At. Data Nucl. Data Tables* **38** 1–197

Schaupp D, Schumacher M, Smend F, Rullhusen P and Hubbell J H 1983 Small-angle Rayleigh scattering of photons at high energies: Tabulations of relativistic HFS modified atomic form factors *J. Phys. Chem. Ref. Data* **12** 467–512

Schmickley R D and Pratt R H 1967 K-, L-, and M-shell atomic photoeffect for screened-potential models *Phys. Rev.* **164** 104–16

Scofield J H 1973 Theoretical photoionization cross sections from 1 to 1500 keV *Lawrence Livermore Laboratory Report* UCRL-51326

——1985 Private communication to E B Saloman and J H Hubbell

Seltzer S M 1993 Calculation of photon mass energy-transfer and mass energy-absorption coefficients *Radiat. Res.* **136** 147–70

Seltzer S M and Hubbell J H 1995 Tables and graphs of photon mass attenuation coefficient and mass energy-absorption coefficients for photon energies 1 keV to 20 MeV for elements $Z = 1$ to 92 and some dosimetric materials, appendix to invited plenary lecture by J H Hubbell '45 years (1950–1995) with x-ray interactions and applications' *51st National Meeting of the Japanese Society of Radiological Technology (Nagoya, Japan)* (Kyoto: Japanese Society of Radiological Technology) (translation into Japanese by Dr Hisashi Maekoshi)

Sommerfeld A 1920 Bemerkungen zur Feinstructur der Röntgenspektren *Z. Phys.* **1** 135–46

——1934 *Atomic Structure and Spectral Lines* 3rd edn (London: Methuen) p 257

Sørenssen A 1965 The influence of electron screening on high-energy bremsstrahlung and pair production *Nuovo Cimento* **38** 745–70

——1966 Theoretical total cross sections for high-energy nuclear-field pair production in light elements *Nuovo Cimento* **41** 543–58

Stern E A 1974 Theory of the extended x-ray-absorption fine structure *Phys. Rev.* B **10** 3027–37

Storm E and Israel H I 1970 Photon cross sections from 1 keV to 100 MeV for elements $Z = 1$ to $Z = 100$ *Nucl. Data Tables* **7** 565–81

Strutt J W (Lord Rayleigh) 1871 On the light from the sky, its polarization and colour *Phil. Mag.* (4th ser) **41** 107–20, 274–9

——1881 On the electromagnetic theory of light *Phil. Mag.* (5th ser) **12** 81–101

Thomas L H 1927 The calculation of atomic fields *Proc. Camb. Phil. Soc.* **23** 542–8

Thomson J J 1906 *Conduction of Electricity Through Gases* (London: Cambridge University Press) p 325

Tseng H K and Pratt R H 1972 Screening effects in atomic pair production below 5 MeV *Phys. Rev.* A **6** 2049–56

——1980 Screening effects in pair production near threshold *Phys. Rev.* A **21** 454–7

Veigele Wm J 1973 Photon cross sections from 0.1 keV to 1 MeV for elements $Z = 1$ to $Z = 94$ *At. Data Tables* **5** 51–111

Victoreen J A 1943 Probable x-ray mass absorption coefficients for wave-lengths shorter than the K critical absorption wave-length *J. Appl. Phys.* **14** 95–102

——1948 The absorption of incident quanta by atoms as defined by the mass photoelectric absorption coefficient and the mass scattering coefficient *J. Appl. Phys.* **19** 855–60

——1949 The calculation of x-ray mass absorption coefficients *J. Appl. Phys.* **20** 1141–7

Wheeler J A and Lamb W E 1939 Influence of atomic electrons on radiation and pair production *Phys. Rev.* **55** 858–62 (erratum **101** 1836 (1956))

White G R 1952 X ray attenuation coefficients from 10 keV to 100 MeV *NBS Report* 1003

White Grodstein G R 1957 X-ray attenuation coefficients from 10 keV to 100 MeV *NBS Circular* 583

Young A T 1982 Rayleigh scattering *Phys. Today* January, 42–8

Zhou B, Kissel L and Pratt R H 1992 Simple computational schemes for x-ray anomalous scattering factors for ions *Nucl. Instrum. Methods* B **66** 307–12